

Geophysics

By John D. Hendricks

Geophysical studies conducted within the East Mojave National Scenic Area (EMNSA) include gravity and aeromagnetic surveys on a regional scale, local electrical (induced polarization, telluric, and audio magnetotelluric) traverses, a limited number of heat-flow measurements, and airborne radiometric measurements. Each of these methods has a particular application in assessing the mineral potential of the area.

In general, gravity anomalies, when analyzed for regions the size of the study area, will yield information as to (1) the rock-density distribution within the crust, (2) the isostatic state of the region, and (3), when combined with other geophysical data, the nature of the lower crust and upper mantle. Although the isostatic state and nature of the lower crust and upper mantle are important in understanding the genesis of mineral deposits in a region, they do not have a direct application to the resource potential in the upper crust. In order to eliminate the gravitational effects arising from deep sources, the isostatic anomaly (Jachens and Griscom, 1982) will be used in describing gravity anomalies in the EMNSA.

In contrast to gravity anomalies, magnetic anomalies arise strictly from sources in the upper crust and, in this part of the Basin and Range Province, represent susceptibility contrasts of less than about 15 km in depth. Magnetic variations result primarily from differences in magnetite content and in the inherent or remanent magnetization of a particular rock body. Analysis of the magnetic patterns in the study area are helpful in delineating buried contacts between varying rock units, the location and attitude of fault zones, the depth to basement beneath sedimentary cover, and, at least in one case, the presence of substantial iron and iron-related deposits.

Electrical traverses have been conducted in the Providence Mountains (Miller and others, 1985; Goldfarb and others, 1988) to delineate the extent of alteration and sulfide mineralization along the East Providence and Bighorn fault systems (pl. 1).

Heat-flow measurements obtained within the EMNSA are part of a broad regional survey of the southern Basin and Range Province (J.H. Sass and others, unpub. data, 1990). When viewed over a large area, the EMNSA shows values in the range of about 80 to 100 mW/m² (milliwatts per square meter), which are fairly typical of the region. Heat-flow measurements are important to an understanding of the thermal history of the region. However, currently available spacing of the individual measurements does not allow us to make direct comparisons with individual geologic features.

Airborne radiometric measurements were conducted throughout the region as part of the National Uranium Resource Evaluation Program (NURE). These measurements are sensitive to concentrations of U, K, and Th. Results of this survey are discussed in the subsection below entitled "Aerial Gamma-Ray Surveys."

Gravity Survey

Gravity data for the EMNSA and surrounding areas were obtained from Snyder and others (1982), Miller and others (1986), and Mariano and others (1986). The observed gravity data were reduced to the free-air anomaly. Bouguer, curvature, and terrain corrections, using a density of 2.67 g/cm³, were added to obtain the complete Bouguer anomaly. To eliminate that part of the Bouguer field that arises from deep sources, a regional field was subtracted from the Bouguer anomaly using the method described by Jachens and Griscom (1982). The resulting isostatic anomaly (pl. 4) will be used below in the description of specific gravity features.

A relatively straightforward relation exists between the isostatic anomaly and rock types as mapped within the study area (pl. 4). In general, isostatic "highs" are present in areas consisting predominantly of Proterozoic metamorphic rocks and Jurassic granitoids; intermediate values, in regions of Cretaceous plutonic rocks; and "lows," in areas of thick deposits of Tertiary volcanic rocks and Tertiary and Quaternary surficial deposits. Density measurements presented by Miller and others (1986) and Wilshire and others (1987) indicate, from samples collected in the New York Mountains and Cinder Cone lava beds area, that Proterozoic schist and gneiss average 2.674±0.07 g/cm³; Mesozoic intrusive rocks (adamellite or monzogranite, and granite), 2.60±0.02 g/cm³; and unspecified Tertiary volcanic rocks, a wide range that averages 2.456±0.40 g/cm³. In addition, two samples of Proterozoic amphibolite have densities of 2.96 and 3.10 g/cm³.

Magnetic Survey

Data used to produce the aeromagnetic map (pl. 5) were collected during three separate surveys: in California, (1) the Kingman-Trona area (U.S. Geological Survey, 1983) and (2) the Needles $1^{\circ} \times 2^{\circ}$ quadrangle (U.S. Geological Survey, 1981); and in Nevada, (3) part of the Kingman $1^{\circ} \times 2^{\circ}$ quadrangle (Oliver and others, 1986). In all of these surveys, a flight height of 1,000 ft (304 m) above average terrain was employed. Because of the irregularity of the local topography, however, the actual height above ground varied from about 400 ft (122 m) to 2,500 ft (762 m) (Miller and others, 1986). In the California surveys, flight-line spacing was 0.5 mi (0.8 km), whereas spacing averaged 1.0 mi (1.6 km) in Nevada. The California and Nevada surveys have been merged to eliminate any effects caused by the differing survey parameters. The standard (uniform) Earth's magnetic field has been subtracted from the observed measurements to yield the residual-magnetic field.

Within the EMNSA, regions show diverse residual-magnetic characteristics (pl. 5). These regions generally fall into three types of magnetic patterns: (1) low-amplitude (>200 nanoTesla (nT)), low-gradient highs and lows, (2) intermediate- to large-amplitude (200–500 nT), intermediate-gradient highs and lows, and (3) intermediate-amplitude (100–300 nT), steep-gradient complex anomalies. In general, these three anomaly patterns can be related to rock type or geologic environment. Type-1 patterns correspond to alluvium-filled valleys and areas of predominantly Cretaceous granite; type-2 anomalies correlate with exposures of Proterozoic metamorphic rocks and Jurassic granitoids; and type-3 anomalies are present in areas that comprise mostly Tertiary and Quaternary, mafic to silicic lava flows, vents, and pyroclastic materials. The magnetic signature of a region not only depends on the magnetic character of the rocks but also the depth to the source. For example, in a deep basin the basement rocks may be quite magnetic, but, because of the increased distance between sensor and source and the nonmagnetic character of the intervening basin fill, the amplitudes and gradients of anomalies will be reduced and the magnetic signature may be quite different from areas where similar source rocks are near the surface. Two isolated magnetic anomalies of particular note in the EMNSA are associated with the Vulcan iron-skarn deposit and the Woods Mountains caldera (McCurry, 1988).

Discussion of Gravity and Magnetic Anomalies

Interpretation of the gravity and magnetic maps (pls. 4 and 5, respectively) are summarized from a series of relatively recent U.S. Geological Survey Wilderness Bulletins and Miscellaneous Field Studies Maps. Interpretations included in four additional geologic and geophysical studies pertaining to the region also contributed significantly to this report (Carlisle and others, 1980; Beckerman and others, 1982; DeWitt and others, 1984; McCurry, 1988). Although these studies are for the most part not adjoining, they do cover a large part of the area, and so the geophysical interpretations can be projected across intervening regions. In addition to this summary of previous work, a brief discussion of the gravity and magnetic characteristics of the southern Clark Mountain Range and Woods Mountains caldera is presented.

Ivanpah Valley and New York Mountains

Isostatic-gravity values range from a high of about -12 mGal over the central New York Mountains to a low of -40 mGal in the Ivanpah Valley (pl. 4). The highest values are associated with outcrops of Proterozoic schist and gneiss, whereas the lowest values are present over unconsolidated basin-fill materials in Ivanpah Valley. The thickness of alluvium in Ivanpah Valley is in excess of 1,980 m, as shown by cuttings and drill-hole logs from the Ivanpah Partnership "Ivanpah 13" drill hole (Hodgson, 1980). On the basis of detailed gravity, magnetic, and seismic surveys (Carlisle and others, 1980), the maximum sediment thickness is about 2,440 m on the east side of the valley. The north-northwest-striking Ivanpah fault cuts across the valley from the vicinity of Mountain Pass to the general area of the Vanderbilt Mine (pl. 2). Seismic information provided by Carlisle and others (1980) suggested that vertical offset is approximately 366 m in the center of the valley near the Morningstar Road (pl. 1). The series of northwest-striking faults in the area of the Vanderbilt Mine generally correspond to a change in the type of basement rocks from Proterozoic schist and gneiss on the northeast to the informally named, Cretaceous Mid Hills adamellite of Beckerman and others (1982) (unit Kmh, pl. 1) on the southwest. This change is marked by a steep gravity gradient, decreasing to the southwest, that has

a variation of about 20 mGal. Gravity values also decrease toward the south and southeast from the northern New York Mountains, attributed to a southward-thickening wedge of volcanic rocks, gravel, and alluvium that cumulatively attain a thickness of a few thousand feet in Lanfair Valley (Miller and others, 1986). A gravity decrease that is present between the north-central part of the New York Mountains and the town of Nipton cannot be explained by examination of surface exposures. This decrease is probably due to an unexposed felsic intrusion of unknown age or perhaps thrust faults or detachment faults that penetrate Proterozoic basement and juxtapose Proterozoic rocks over Tertiary basin fill (Miller and others, 1986). However, Proterozoic rocks are not known to be thrust over Tertiary rocks in any of the mountain ranges of the EMNSA.

Magnetic-anomaly values in this area range from highs of slightly more than +200 nT to lows in excess of -200 nT. Anomalies over Proterozoic rocks are broad, having amplitudes of about 100 nT. Three such positive anomalies are present in the Ivanpah Valley. Two of them, in the southwestern and southeastern part of the valley, are roughly circular; Carlisle and others (1980) suggested that the tops of the sources are approximately 975 m below the surface, which would place these tops beneath the interface between basement and sedimentary deposits. The third is a positive ridge that trends north along the west side of the valley. Depth-to-source estimate for this anomaly is 1,738 m (Carlisle and others, 1980). The magnetic signature in areas of exposed Proterozoic rocks suggests that metamorphism or hydrothermal alteration has affected the magnetite content of the rocks (Miller and others, 1986). The positive anomalies in Ivanpah Valley may, therefore, represent relatively unaltered Proterozoic basement sources. Volcanic rocks exposed along the southeast margin of the New York Mountains near Barnwell (pl. 1) produce high-amplitude, short-wavelength anomalies, which indicate strongly the magnetic character of the rocks. In the New York Mountains, a change from Proterozoic schist and gneiss on the northeast to Cretaceous adamellite on the southwest corresponds to a down-to-the-northeast magnetic gradient. This change in magnetic intensity corresponds, but is opposite in sense, to the gravity gradient discussed earlier, which would imply that the Mid Hills adamellite is less dense, but more magnetic, than the adjacent Proterozoic metamorphic rocks. The reduced magnetic character of the Proterozoic rocks may reflect extensive alteration of magnetite in these rocks. However, the reduced magnetic character could also result from either metamorphism under low-oxygen-fugacity or reducing conditions or, perhaps, high-sulfur-fugacity conditions such that most of the iron is tied up in iron-magnesium silicates or pyrite rather than magnetite (D.A. John, written commun., 1993).

Lanfair Valley and Piute Range

The Lanfair Valley and Piute Range area is characterized by large magnetic anomalies and a relatively flat isostatic-gravity field. A northeast-trending belt of positive magnetic anomalies extends from Fenner Valley on the southwest through the Vontrigger Hills and southern Piute Range, terminating some 6 mi (10 km) east of the central Piute Range. An apparent westerly oriented arm of this pattern connects the Grotto Hills and Lanfair Buttes region to the central part of the northeast-trending belt of positive anomalies. These positive anomalies correlate well with outcrops of Proterozoic crystalline rocks. Southeast of this magnetic ridge is an area consisting primarily of Mesozoic granitic rocks in the Signal Hill and Homer Mountain areas. The region here is characterized by a series of magnetic lows. The contact between these two units is largely concealed beneath volcanic and alluvial deposits of the southern Lanfair Valley and may correspond to the abrupt magnetic change between the magnetically high and low areas (Nielson and others, 1987). The northern Piute Range and Castle Mountains contain extensive volcanic vents and associated rocks, and the magnetic field shows a number of sharp, large-amplitude highs and lows. In the vicinity of Hart Mining District (pl. 2), near the northeast corner of the EMNSA, the magnetic field is fairly subdued, although this area also contains extensive volcanic materials similar to those exposed in the Piute Range. The relatively smooth magnetic field here may represent a topographic effect because the area is lower and not as rugged as the Piute Range; this results in a more constant survey height. Alternatively, highly magnetic volcanic vents may possibly be absent in the immediate vicinity.

The isostatic-gravity field in this region is relatively smooth, showing a general decrease into Lanfair Valley. On the basis of one station, low closure of about 5 mGal over the Lanfair Buttes probably represents a sequence of alluvial and volcanic materials as much as 1 km thick. A similar anomaly is present near the junction of Ivanpah and Hart Mine roads (pls. 4 and 5). Small gravity highs are present over the Vontrigger Hills and south

of the Grotto Hills. These anomalies probably represent the thinning or absence of Cenozoic sedimentary or volcanic cover.

Mid Hills, Providence Mountains, and Southern Providence Mountains

In the New York Mountains and northern Mid Hills, gravity and magnetic anomalies are relatively smooth and flat (pls. 4, 5), thereby highlighting the overall uniform character of the informally named Mid Hills adamellite of Beckerman and others (1982). South of Cedar Canyon, however, both gravity and aeromagnetic maps show large changes and numerous closures, reflecting the mixture of Proterozoic metamorphic rocks, Mesozoic intrusions, Tertiary volcanic rocks, and Tertiary sedimentary rocks. A large (-400 nT), arcuate magnetic low extends from the Grotto Hills to the Cedar Canyon Fault in the Mid Hills (pl. 5). This feature probably results from both a thickened Tertiary and Quaternary volcanic and (or) sedimentary sequence and dipolar lows associated with positive anomalies to the south. A circular area, some 15 km in diameter, of relatively high magnetic values lies to the south of the large, arcuate low. This area is characterized by outcrops of both Proterozoic and Mesozoic crystalline rocks, and the high magnetic anomaly reflects the presence of these rocks at the surface. The westernmost peak in this area of high magnetic values is present over the informally named Black Canyon hornblende gabbro of Beckerman and others (1982) (unit Kbc, pl. 1), which is a circular plug of Cretaceous hornblende gabbro enclosed by the Mid Hills adamellite, some 2 km in diameter. The gabbro here contains as much as 6.5 volume percent opaque minerals, primarily magnetite (Beckerman and others, 1982), resulting in the observed magnetic anomaly. A 5- to 10-mGal gravity anomaly corresponds to the large, magnetically high area. Gravity values in the central and northern Providence Mountains show a general decrease towards the northwest. This gradient probably reflects the general change in the types of rock in the basement from relatively dense Jurassic granitoids in the southeast to the less dense Cretaceous Mid Hills adamellite in the northwest (pl. 1).

The central and southern Providence Mountains are characterized by several large positive magnetic anomalies. The largest of these is associated with the Vulcan iron-skarn deposit. This anomaly (3,500 nT) suggests a possible continuation of the ore body to the east (Goldfarb and others, 1988). Another large magnetic anomaly ($\sim 2,000$ nT) some 6 mi (10 km) to the northeast may represent the presence of an iron skarn and (or) a highly magnetic Jurassic granitoid body. Positive anomalies present in the southern part of the Woods Mountains suggest that the nonmagnetic tuff that makes up the surficial exposures overlies magnetic basement of probable Jurassic age.

The East Providence fault strikes north along the east side of the range (pl. 1). In general, a series of magnetic lows correspond to the surface trace of the fault. Some lows are present over exposures of apparently nonmagnetic Paleozoic sedimentary rocks, whereas others, present in areas of Proterozoic or Jurassic crystalline rocks, may result from hydrothermal alteration of magnetic minerals along the fault. Steep down-to-the-west gravity and magnetic gradients are present 1 to 2 mi (1.6–3.2 km) into Kelso Wash along the west side of the Providence Mountains, suggesting that the east side of the valley is a pediment surface.

Granite Mountains

Isostatic-gravity values in this region range from a high of about -10 mGal to a low of -25 mGal (pl. 4). Areal corresponding magnetic values range from greater than 200 to less than -100 nT (pl. 5). In general, the northern part of the range is characterized by a magnetic low and a positive gravity closure. The southern part of the range shows a gravity minimum and a variable, but generally high, magnetic anomaly. The division between these two geophysically distinct regions is marked by the concave-to-the-southeast Bull Canyon fault (pl. 4). Gravity and magnetic features of the region have been discussed by Howard and others (1987) and are, therefore, only summarized briefly here. The magnetic trough in the northern part of the range corresponds to the Bull Canyon fault and probably reflects topographic effects, low magnetic susceptibility of the unaltered plutonic rocks, and possibly alteration along the fault zone. Gravity anomalies indicate that the predominantly Jurassic basement rocks north of the fault are denser than the mostly Cretaceous granites that crop out to the south of the fault.

The west margin of the Granite Mountains is marked geomorphologically by Budweiser Wash and the corresponding Bristol Mountains fault (pl. 1). Steep gravity gradients here indicate that this fault is a major

structure that juxtaposes less dense Tertiary volcanic rocks of the Old Dad Mountains (2 to 3 km southwest of the EMNSA; see fig. 2) and some sedimentary rocks to the west against Mesozoic crystalline rocks of the Granite Mountains.

North and northwest of the Granite Mountains in the alluvial plain of the Devils Playground, gravity values suggest that the thickness of sedimentary deposits is not greater than about 1,000 ft (305 m), and basement rocks here are probably Mesozoic granitoids. In the western part of this valley, a northwest-trending, 300-nT magnetic ridge is present along the southwest margin of the northern Bristol Mountains (approximately 5 km southwest of the EMNSA; see fig. 2). This anomaly also roughly corresponds to the projection of the Bristol Mountains fault farther to the southeast. The anomaly is fairly broad and has subdued gradients, suggesting that the source lies at some depth below the surface, possibly as much as about 1 mi (1.6 km). The source of this anomaly is not evident from surface observations, and no conspicuous associated gravity anomaly exists. Two possibilities for a source are extensive iron mineralization or intrusion of Tertiary igneous rocks along the fault zone.

Old Dad Mountain and Kelso Mountains

Exposed in the Old Dad Mountain and Kelso Mountains area are a wide variety of rock types that include Proterozoic schist and gneiss, Paleozoic sedimentary rocks, Mesozoic granitoids, Tertiary volcanic rocks, and unconsolidated sediments (pl. 1). The gravity and magnetic patterns are equally complex. The northwest-trending Old Dad Mountain is characterized by both gravity and magnetic highs of as much as 10 mGal and 400 nT, respectively (pls. 4, 5). Along the southwest margin of this mountain, the magnetic gradient is typical of a steeply dipping fault, although some of the gradient probably results from topographic differences. Both the gravity and magnetic anomalies appear to wrap around the south end of Old Dad Mountain and the Kelso Mountains before dying out in Kelso Wash. A prominent arcuate magnetic and gravity trough is present over the Kelso Mountains, which separates the gravity and magnetic highs of Old Dad Mountain from an area of positive anomalies centered north of Kelso Peak. The northwest limb of the trough appears to continue for as much as 30 km, and the northeast limb some 10 km, before merging with lows of Kelso Wash. Because the area of the trough is, for the most part, covered by alluvial deposits, the source of the anomaly is not evident. If these features represent a fault or series of faults, extensive hydrothermal alteration may have taken place along the fault zones, and the area of the trough might have been downdropped; if the anomalies reflect an intrusive contact, alteration may have occurred along this contact, and the rocks underlying the trough are less dense than the surrounding terrane.

Trending due north from Old Dad Mountain and the Kelso Mountains is a very conspicuous linear isostatic-gravity feature (pl. 4). Relief across this feature is about 10 mGal, decreasing to the east. A somewhat similar north-northwest-trending gradient is noted along the northeast side of Shadow Valley. These two conspicuous anomalies intersect at the north end of Shadow Valley. The magnetic pattern is quite similar to the gravity lineation, although the area of the western gravity gradient is represented by a series of sharp magnetic highs and lows that reflect surficial Tertiary basaltic vents and associated volcanic rocks. The gravity gradient along the northeast edge of Shadow Valley has a corresponding magnetic gradient, although the sense of relief is opposite (in other words, a down-to-the-northeast magnetic anomaly). The southern part of the area of the gravity low defined by these two linear anomalies includes extensive exposures of Cretaceous granite. One interpretation is that the granite extends northward beneath sedimentary cover and forms the floor of Shadow Valley. The gravity low, therefore, represents the combined effect of low-density alluvial valley fill and relatively low density basement rocks. Small outcrops of pre-Tertiary rocks have been noted in Shadow Valley (DeWitt and others, 1984). These have no corresponding gravity anomaly, suggesting that the alluvial fill is relatively thin. The magnetic pattern within the valley shows little relief but is a relative high when compared to immediately adjacent terranes; this would be consistent with the above interpretation. A northwest-trending magnetic gradient crosses the valley in the vicinity of Interstate 15. This linear feature may mark either a lithologic change in the Cretaceous granitoid suite or a subsurface fault with down-to-the-northeast displacement.

Clark Mountain Range

Lying between the Ivanpah and Shadow Valleys, the Clark Mountain Range is a structurally and lithologically complex block that consists of Early Proterozoic metamorphic rocks, Middle Proterozoic igneous

intrusions, and Paleozoic to Mesozoic sedimentary units (pl. 1). The east side of the range is characterized by a structurally complex, diverse assemblage of Proterozoic metamorphic and igneous rocks, while the western part of the range is characterized by a relatively thick section of Phanerozoic sedimentary rocks that has been thrust over the basement complex. Both gravity and magnetic anomalies indicate that the Proterozoic rocks continue to the east at shallow depths nearly to the center of Ivanpah Valley (pls. 4, 5). The trend of the anomalies in the western part of Ivanpah Valley is north-south, which is at an angle of approximately 20° to the north-northwest structural grain of the surrounding region. In the western Clark Mountain Range, geophysical anomalies follow the regional structural trends.

Isostatic-gravity values in this region range from lows of about -40 mGal in the Ivanpah and Shadow Valleys to a high of approximately -10 mGal over the eastern range front near the intersection of Interstate 15 and the Ivanpah Road. Gravity values show a gentle decrease westward across the range until sharp gradients associated with Shadow Valley are encountered. The apparent smoothness of the isostatic anomaly is due, in part, to the relatively wide spacing of gravity stations within the range. Small features, such as igneous dikes and plugs in the general area of Mountain Pass, cannot be detected with the available survey, even though large density contrasts may exist between rock units. Lower gravity values in the western part of the Clark Mountain Range are due, in part, to the presence of a sequence of Paleozoic sedimentary rocks that may have a total thickness of as much as 2.5 km.

The residual-magnetic anomaly shows a large amount of relief within the Clark Mountain Range in contrast to the isostatic gravity. Although some magnetic variation may result from topographic effects, a series of highs and lows in the southern part of the range cannot be accounted for by the varying distance between the aircraft and ground surface. Traversing from east to west across the southern part of the mountains, the broad magnetic high in western Ivanpah Valley probably represents a magnetite or pyrrhotite component of the Proterozoic basement there. This anomaly continues from the southern Ivanpah Valley northward, generally conforming to the shape of the margins of the valley. Immediately to the west of this high, an elongate magnetic low closure of about -80 nT, which shows gradients similar to the above high, is present. This low corresponds to the subsurface projection of the Ivanpah fault (Burchfiel and Davis, 1971) and may indicate the presence of hydrothermal alteration along the fault zone. A magnetic high extends from immediately northwest of Mountain Pass some 10 km to the south-southeast. Gradients associated with this anomaly suggest a shallow source, and the anomaly appears to be related to a series of Middle Proterozoic ultrapotassic rocks and carbonatite exposed in the area. These rocks are the host for the rare earth element deposits of Mountain Pass. To the west of this magnetic ridge, a northwest-oriented low of about -100 nT is present. The location and trend of this anomaly appear to correspond to a series of thrust faults that are exposed in the western Clark Mountain Range and Ivanpah Mountains, and the low may represent a thrust stacking of Paleozoic sedimentary rocks on Proterozoic basement. A +200-nT magnetic anomaly is present in the southwestern Clark Mountain Range, Mescal Range, and Striped Mountain areas. The source of this anomaly is not obvious from surface exposures; gradients, however, indicate that the top of the causative body cannot be much more than 1.6 km below the surface and is probably at the top of the Proterozoic basement. Several small outcrops of Mesozoic granitoids are present in this area (pl. 1). When combined, the above anomalies indicate a complex distribution of lithologies and magnetic properties in the southern Clark Mountain Range and northern Ivanpah Mountains. In contrast, the northern Clark Mountain Range is typified by gentle gravity and magnetic gradients, although the region is structurally complex. The gravity anomaly in the northern Clark Mountain Range consists of a gradient that extends southwestward from a high in the southern Spring Mountains (20 km north of the EMNSA; see fig. 2) to the low in Shadow Valley. A northwest-trending magnetic gradient in this area is present between positive anomalies in the western Ivanpah Valley and a series of lows along the west flank of the Clark Mountain Range.

Woods Mountains Caldera

Two conspicuous features shown on plates 4 and 5 are the negative gravity and magnetic anomalies associated with the late Tertiary Woods Mountains caldera (McCurry, 1988; see also pl. 1). Both anomalies are large-amplitude, circular features that have very steep gradients. These features are in sharp contrast to the

surrounding gravity and magnetic fields. The gravity anomaly is approximately -30 mGal and some 14 km in diameter, while the magnetic anomaly is about -600 nT and about 9 km in diameter. Both features appear to be related to a caldera and (or) an underlying pluton. The presence of sparse Jurassic granitoids within the boundaries of the gravity low at its south margin, the fact that the anomalies are of differing lateral extent, and the fact that centers of the lows do not coincide (the magnetic center is offset some 3 km to the southwest), all indicate that the anomalies do not result strictly from a caldera infilling of low-density and low-susceptibility, low-remnant-magnetization pyroclastic materials. Most granitoids on the west and north sides of the anomalies are Cretaceous in age. Thus, the negative magnetic anomaly may represent the true size and geometry of the actual caldera, which, as was shown by McCurry (1988, figs. 1, 2), is a “trap door” feature that has the western and southwestern parts downdropped more than the eastern parts, which results, therefore, in a west-dipping, relatively smooth caldera floor. Structural relief along the west caldera margin may be somewhat in excess of 1 km, although the size of this relief is relatively small when compared to the relief at other well-exposed calderas (D.A. John, written commun., 1993).

The associated gravity anomaly of the Woods Mountains caldera extends well beyond the surficial bounds of this feature (pl. 4). This indicates that a negative density contrast, which occupies an area larger than the surface expression, must be present in the subsurface. Positive magnetic anomalies are present peripheral to the magnetic low but are within the area of the negative gravity anomaly.

The gravity low probably represents intrusion of a relatively low density granitic stock into Jurassic and Cretaceous granitoids combined with caldera formation and infilling with low-density pyroclastic materials and rhyolite. The silicic stock in this case would be circular, about 14 km in diameter, and have steeply dipping sides. The magnetic low probably results from filling of the caldera by pyroclastic materials and by nonmagnetic silicic lava. Positive magnetic anomalies peripheral to the magnetic low but within the gravity anomaly would reflect the presence of magnetic Jurassic and Cretaceous granitoids left above the intrusion. These granitoids may have been remagnetized during the Tertiary magmatic event.

Aerial Gamma-Ray Surveys, by Joseph S. Duval

Aerial gamma-ray surveys measure the gamma-ray flux produced by the radioactive decay of the naturally occurring elements potassium (^{40}K), uranium (^{238}U), and thorium (^{232}Th) in the top few inches of rock or soil (Duval and others, 1971). If the gamma-ray system is properly calibrated (see for example, Grasty and Darnley, 1971), the data can be expressed in terms of the estimated concentrations of the radioactive elements. Data for potassium are usually expressed as concentrations in units of percent potassium (percent K); thorium, as parts per million equivalent thorium (ppm eTh); and uranium, as parts per million equivalent uranium (ppm eU). The term equivalent is used because the technique actually measures the gamma-ray flux from the decay of thallium (^{208}Tl) and bismuth (^{214}Bi), which are decay products of ^{232}Th and ^{238}U , respectively, and also because the possibility of radioactive disequilibrium exists in the thorium and uranium decay series.

During the period from 1975 to 1983, the U.S. Department of Energy carried out the National Uranium Resource Evaluation (NURE) Program, which included aerial gamma-ray surveys of most of the conterminous United States. Figure 34 shows the $1^\circ \times 2^\circ$ National Topographic Map Series quadrangles from which data (U.S. Department of Energy, 1979a, b, c, 1980) were taken for this study. Although many airborne gamma-ray systems used to make these surveys were calibrated, many early surveys were done without calibration and were not converted to the concentrations of the radioactive elements. Detailed examinations of the digital data available on magnetic tape also showed that many “calibrated” surveys do not match the data from “calibrated” surveys of adjacent areas. For these reasons, the data must be corrected to obtain a consistent data base. Duval and others (1989, 1990) discussed the types of corrections applied to the data and provided index maps that indicate the specific kinds of corrections applied to the data sets used in this work.

The NURE aerial gamma-ray data were collected by several private contractors using “high-sensitivity” gamma-ray systems. These systems used sodium-iodide detector crystals that have detector volumes of $2,000\text{--}3,300\text{ in}^3$ ($33,000\text{--}54,000\text{ cm}^3$). All systems included electronic navigation equipment, radar altimeters, magnetometers, and “upward-looking” gamma-ray detectors. The upward-looking detectors were partially shielded from radiation coming from the ground by either placing them on top of the other detectors or by using

lead. The upward-looking detectors measure the amount of radiation from ^{214}Bi in the atmosphere, which is used to correct the estimated ground concentrations of ^{238}U . The data were corrected by the contractors for background radiation due to aircraft contamination and cosmic rays, Compton scattering effects, altitude variations, and airborne ^{214}Bi . The gamma-ray surveys were flown at a nominal altitude of 122 m above the ground. The gamma-ray systems were calibrated using the calibration pads at Grand Junction, Colo. (Ward, 1978), and the dynamic test strip at Lake Mead, Ariz. (Geodata International, Inc., 1977). The nominal flight-line spacings for the surveys were 1.6 to 4.8 km and included tie lines flown approximately perpendicular to the flight lines at intervals of 25 to 29 km. Contoured plots of K, eTh, and eU for the EMNSA and its surrounding area are shown in figure 35.

Table 8 lists the estimated average concentrations of potassium, uranium, and thorium for some of the geologic units that crop out in the EMNSA. The values listed in table 8 were determined by inspection of gamma-ray profiles (fig. 35) overlain on the geologic map (pl. 1), but not all geologic units found in the study area are included in table 8 because of little or inadequate data over some units. Average potassium concentrations range from 0.5 to 3.5 percent K. The highest values (>2.9 percent K) are present in the following map units (pl. 1): Jurassic quartz monzonite of Goldstone (Jgo); informally named, Jurassic Ivanpah granite of Beckerman and others (1982) (Ji); informally named, Cretaceous Mid Hills adamellite of Beckerman and others (1982) (Kmh); younger Tertiary volcanic rocks (Tv_1); Tertiary Wild Horse Mesa Tuff of McCurry (1988) (Tw); Tertiary Tortoise Shell Mountain Rhyolite of McCurry (1988) (Tts); and Early Proterozoic intermediate-age granitoids (Xg_2). As pointed out by Beckerman and others (1982), the K_2O contents determined for the Mid Hills adamellite and Ivanpah granite commonly range from 3.5 to 4.8 and 5.0 to 9.0 weight percent, respectively, and seem to corroborate the potassium concentrations sensed remotely by the aerial gamma-ray surveys. The lowest average potassium concentration (0.5 weight percent K) coincides with Cambrian dolomite (€d). Average uranium concentrations range from 1.5 to 4.4 ppm eU. The highest values (>3.5 ppm eU) are present in the following units: Quaternary eolian sand deposits (Qes); Quaternary playa deposits (Qp); younger Tertiary volcanic rocks (Tv_1); Tertiary dacite and rhyolite (Tdr); Tertiary Tortoise Shell Mountain Rhyolite (Tts); and Mesozoic volcanic and sedimentary rocks (Mzv). The lowest average uranium values (<2 ppm eU) are present in Jurassic felsic rocks of Colton Hills (Jch), Cambrian dolomite (€d), and Late Proterozoic and Cambrian siliciclastic rocks (€Zs). Average thorium concentrations range from 3.0 to 31.0 ppm eTh. The highest values (>17 ppm eTh) are present in Quaternary eolian sand deposits (Qes); Quaternary playa deposits (Qp); Tertiary dacite and rhyolite (Tdr); informally named, Cretaceous Teutonia adamellite of Beckerman and others (1982) (Kt); Jurassic Ivanpah granite (Ji); and Early Proterozoic migmatite (Xm). The lowest average thorium values (<7 ppm eTh) are present in Quaternary eolian sand deposits (Qes); Jurassic(?) Sands Granite (Js); Cambrian dolomite (€d); and Late Proterozoic and Cambrian siliciclastic rocks (€Zs).

Anomalously high thorium concentrations also are present at two locations that were not listed in table 8 because the flight lines pass near the contacts between different geologic units and so the data could not be positively assigned to a particular unit. The first of these locations has a maximum value of 42 ppm eTh; the flight line passes near an outcrop of Middle Proterozoic granitic rocks, located approximately at lat $35^{\circ}29'\text{N}$. and long $115^{\circ}32'\text{W}$. This same location has high uranium values, greater than 7 ppm eU, and some potassium values greater than 4 percent K. The second area of anomalously high thorium values is present near a patch of Jurassic Ivanpah granite (Ji), located approximately at lat $35^{\circ}22'\text{N}$. and long $115^{\circ}30'\text{W}$. Another anomalously high potassium value of greater than 5 percent K is present in a small mass of Jurassic quartz monzonite of Goldstone (Jgo) near lat $34^{\circ}56'\text{N}$. and long $115^{\circ}32'\text{W}$.

The ratios of K/eTh, eU/K, and eU/eTh were examined for anomalies that can indicate a relative enrichment of one or more elements. Enrichment of potassium and (or) uranium can be indicative of alteration processes that are associated with various types of mineralization. Enrichment of thorium can be indicative of the presence of the heavy mineral monazite, which may contain rare earth elements.

An anomalous K/eTh ratio of 0.72, indicative of a relatively enriched potassium content, is present in Early Proterozoic younger granitoids (Xg_1) near lat $35^{\circ}4'\text{N}$. and long $115^{\circ}7'30''\text{W}$. This anomaly is located in the vicinity of an occurrence of polymetallic veins. Similarly anomalous K/eTh ratios ranging from 0.3 to 0.5 are also present over parts of the informally named, Cretaceous Live Oak Canyon granodiorite of Beckerman

and others (1982) (Klo). One outcrop near lat 35°17'N. and long 115°16'W. is known to have a tungsten-skarn deposit (pl. 2). Limited amounts of data over a large mass of Jurassic quartz monzonite of Goldstone (Jgo) in the vicinity of lat 34°52'N. and long 115°34'W. have anomalous K/eTh ratios that range from 0.3 to 0.5. This mass of Jurassic quartz monzonite of Goldstone is known to host numerous mineral occurrences of various types (pl. 2). Other apparently anomalous K/eTh ratios ranging from 0.3 to 0.7 are present in Quaternary eolian sands (Qes) near lat 34°55'N. and long 115°44'W. The high ratios are caused by the low thorium concentration (about 4.4 ppm eTh) of the eolian sands.

Various eU/K and eU/eTh ratio anomalies also are present in the EMNSA. One eU/K ratio anomaly that has values of 4.5 to 5.9 is present approximately at lat 36°54'N. and long 115°36'W. This anomaly is apparently associated with Tertiary gravel (Tg), but its significance is unknown. Approximately at lat 34°56'N. and long 115°34'W., a similar eU/K ratio anomaly is present in Devonian to Permian limestone (PDI). At this location, the uranium concentration is a moderate value of about 2 ppm eU, which suggests that the apparently anomalous concentration is likely to be characteristic of the limestone. Near lat 35°4'N. and long 115°11'W., anomalies of eU/K ratio of 4.4 and eU/eTh ratio of 0.8 are present in Tertiary younger volcanic rocks (Tv1). The radioelement concentrations at the anomaly location are 1.5 percent K, 7 ppm eU, and 8 ppm eTh. The potassium and thorium values can be considered as moderate, but the uranium value is relatively high and should be considered anomalous. Other high eU/K ratios ranging from 2.5 to 4.8 are present along a section of a north-south flight line, at long 115°32'W. from lat 35°25'N. to lat 35°29'N.; eU/eTh ratios are as high as 1.4 at some places along the same section of flight line. This section of flight line crosses various rock types.

In conclusion, the NURE gamma-ray data available for the study area provide limited measurements of the potassium, uranium, and thorium concentrations of the various geologic units present on the surface. Some concentrations of potassium are consistent with measured potassium contents of exposed plutonic rocks. The most prominent thorium anomalies are likely to be associated with the carbonatite-related, rare earth element deposits at Mountain Pass, just outside the EMNSA. The ratio data also show a number of interesting anomalies, and some of them may be related to mineral occurrences. A more detailed gamma-ray survey would provide more site-specific information that could then be more closely related to the geology and mineral occurrences.

Landsat Thematic Mapper Surveys, by Marguerite J. Kingston, Shirley L. Simpson, and Martha S. Power

One-quarter of a Landsat Thematic Mapper (TM) scene was processed to be used as a guide for mapping various lithologic units in the EMNSA and to highlight the general distribution of possible areas of hydrothermal alteration. For the preliminary results described in this section, a color-ratio-composite image was produced by digital image processing and interpreted by inspection (fig. 36).

A TM scene, recorded June 6, 1986, was selected for the study because the sun angle is highest at the time of the summer solstice, and so shadowing in this area of high topographic relief is minimized. Landsat TM imagery has 30-m spatial resolution. Data are recorded in six spectral bands or channels in the visible and near infrared; they have excellent radiometric and geometric characteristics. The wavelength coverage of each TM band is as follows:

<i>TM Bands</i>	<i>Wavelength coverage (in micrometers)</i>
1	0.45–0.52
2	0.52–0.60
3	0.63–0.69
4	0.76–0.90
5	1.55–1.75
6	(Thermal infrared, not used in this study)
7	2.08–2.35

Color composite images display color variations that indicate differences in spectral radiance recorded by the Landsat TM from surface materials. Ratioing of selected bands minimizes the influence of topography and enhances spectral differences. Color compositing of three stretched ratios to form color-ratio-composite (CRC) images of TM data allows the detection of specific minerals, which show up as unique colors on the color image. Rocks and soils that are mineralogically and spectrally similar possibly may not be discriminated.

The CRC image of the EMNSA (fig. 36) was produced by combining ratios of TM bands 5:7 (red), 3:1 (green), and 3:4 (blue) according to the techniques of Knepper and Simpson (1992). The resulting colors, used for identification of minerals or mineral groups that may be associated with hydrothermal alteration, are summarized in table 9.

A working copy of a color print was prepared of the CRC image at a scale of 1:100,000, so that it could be overlaid on various geophysical and geologic maps of the EMNSA. Unfortunately, nuances of color and tonal differences were lost in the color paper copy, necessitating referral to the original color transparency to better interpret the CRC image.

In the CRC image, a contribution by a color filter indicates a high ratio value relative to other materials in the scene; thus, red is due to high TM 5:7 ratio values and represents vegetation, which has a strong H₂O absorption in the region of band 7. The TM 3:4 ratio expresses the increase in reflectance from the chlorophyll-absorption band in TM 3 to the near-infrared reflectance plateau in TM band 4, so that the blue color component is very low for vegetated areas. Carbonate minerals and hydroxyl-bearing minerals such as muscovite, kaolinite, or jarosite, which may be associated with hydrothermal alteration, should result in a magenta color owing to the combination of a high value for TM 5:7 ratio (red) and a moderate value for TM 3:4 ratio (blue). However, most hydrothermally altered rocks that contain hydroxyl-bearing minerals are also limonitic, so that the magenta color usually designates only carbonate-mineral-bearing units. The TM 3:1 ratio is coded green and defines rocks and soil that contain ferric iron (limonite). Yellow, the result of combining red and green, appears where TM 5:7 ratio value (red) is high owing to the presence of carbonate or hydroxyl-bearing minerals, as well as where TM 3:1 ratio value (green) is high owing to ferric-iron-bearing minerals such as limonite. White areas indicate a high value in all three component ratios, which is most indicative of the presence of many alteration minerals, especially jarosite, which strongly contributes to the overall radiance.

The detection of limonite traditionally has been important to remote sensing for hydrothermal alteration. As defined by Blanchard (1968), limonite is a general term for hydrous ferric-iron oxides and hydroxides. These minerals absorb strongly in the visible region near TM bands 1 and 4. Limonite may be associated with hydrothermally altered rocks as a result of weathering of pyrite or hematite or other iron-bearing minerals. Gossans typically have an intense ferric-iron absorption. However, some limonite may also be disseminated in sedimentary, volcanic, or metamorphic rocks, unrelated to any epigenetic hydrothermal alteration. Field evaluation is needed to absolutely distinguish hydrothermally altered rocks from those that may only include some limonitic materials from weathering of syngenetic iron-bearing minerals. For example, weathering of biotite and other mafic minerals in granite or metamorphic rocks may produce hematite on some outcrops.

Laboratory spectral-reflectance measurements of representative rock samples collected from the EMNSA were made using a Beckman UV5240 spectrophotometer, using a 100 percent reflectance standard. Four to six representative rock samples were collected from outcrop for the laboratory measurements. Two or three spectral-reflectance measurements were made on the weathered surface of each sample to assure that recorded measurements were consistent, and then the spectral curves were averaged for plotting. Some of these plots of data, which measure spectral reflectance from 400 nm to 2,500 nm to encompass the wavelength range of the TM bands, are reproduced in figures 37 through 48. Note that many unaltered igneous rock samples are spectrally flat, and so they will not show a distinctive color in the image. Also, the red color response of overlying vegetation masks these rocks and any derived soils. The altered samples display deep absorption bands between 2,200 nm and 2,350 nm, which correspond to TM band 7. Carbonate samples typically display absorption features from 2,331 nm to 2,335 nm, which also correspond to band 7.

The most obvious area of alteration in the EMNSA, as defined by the CRC-image color assignments, is in the Castle Mountains, which includes the Hart Mining District (fig. 36; see also pl. 2). Clusters of white pixels are surrounded by yellow and green pixels. Similar areas of alteration represented by the white-to-

yellow clusters of pixels may be in the area of the southeastern Providence Mountains, in the general area of Hidden Hill (fig. 36). Some areas correspond to workings at the Hidden Hill Mine, near the southern tip of the Providence Mountains; others have not been field checked. From the yellow-to-white colors on the CRC image, some areas of alteration appear to be within south-central Hackberry Mountain (fig. 36), where Proterozoic granitoids are in contact with Tertiary volcanic rocks (pl. 1). Some groups of yellow-white pixels correspond with the northern part of Hackberry Mountain, where field checking has confirmed alteration of the volcanic rocks. Another grouping of small numbers of alteration-related pixels is present in the Ivanpah Mountains, where yellow-to-white pixels are displayed in the image on the southern and east slopes. This region includes the recently (1990) active Morning Star Mine (fig. 36; see also pl. 2). Also, small skarn deposits of various types (pl. 2) are located at the contact of carbonate rocks with quartz monzonite on the west slopes of the Ivanpah Mountains and Mescal Range, and these correspond to pixels showing the yellow and white colors.

Small clusters of yellow pixels are spread throughout the alluvial areas. Many may correspond to areas of exposed soil where cattle have frequented wells; others seem to correspond to mine workings, as in the Tungsten Flat area (fig. 36) of the Signal Hill Mining District (pl. 2). However, no widespread exposure of apparently altered rocks exists at these localities.

The magenta color in the CRC image in the area of the northeast slope of the New York Mountains corresponds to outcrops of carbonate rocks that are intruded by granite (fig. 36). This area has also been the site of some skarn-type mineralization.

Granite outcrops in the Granite Mountains, present at low elevations as boulders and unvegetated talus, appear blue in the image. The fracture pattern typical for granite can be seen in the CRC image, both at low and high elevations, but lichen cover at high elevations causes a red color response in the image (fig. 36).

Additional areas in the EMNSA that show a yellow-to-white color on the CRC image need to be field checked in order to determine presence or absence of hydrothermal alteration. Other causes of the color responses in the CRC image may exist. Further processing of the TM data might reveal a more direct correspondence with hydrothermal alteration on the ground, as well as allow a better discrimination of the various rock types that crop out over the EMNSA.

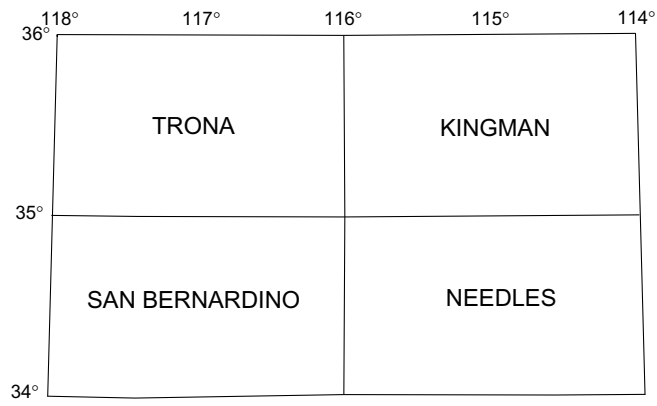


Figure 34. Index map showing 1° x 2° quadrangles from which National Uranium Resource Evaluation Program (NURE) aerial gamma-ray data were taken for study of East Mojave National Scenic Area, Calif. Data for Trona, Kingman, Needles, and San Bernardino quadrangles are from U.S. Department of Energy (1979a, b, c, and 1980, respectively).

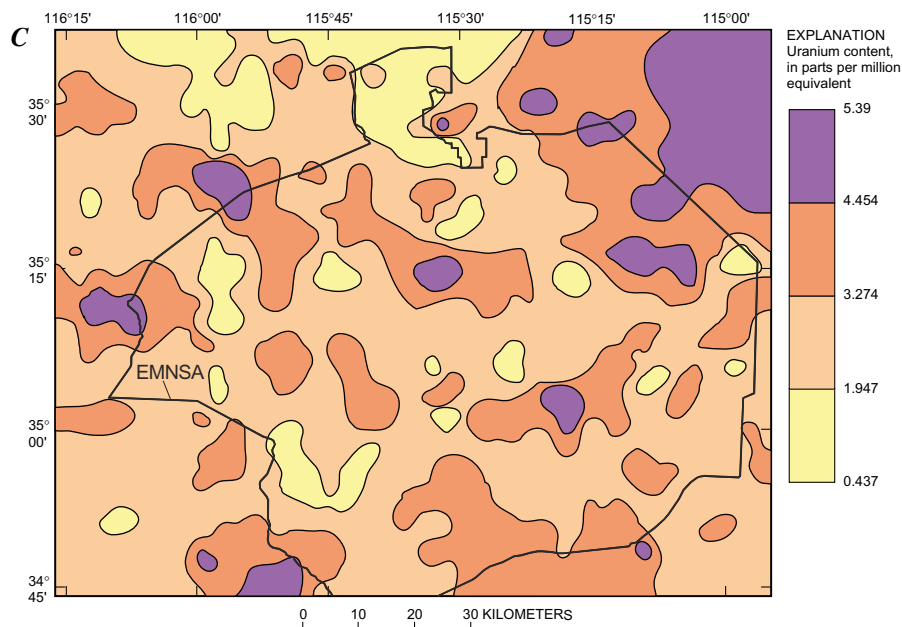
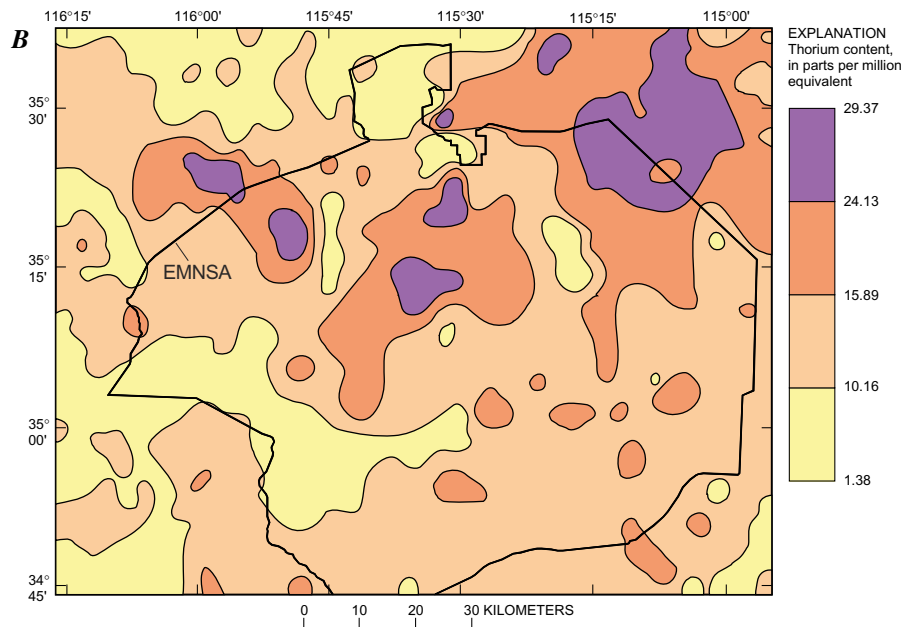
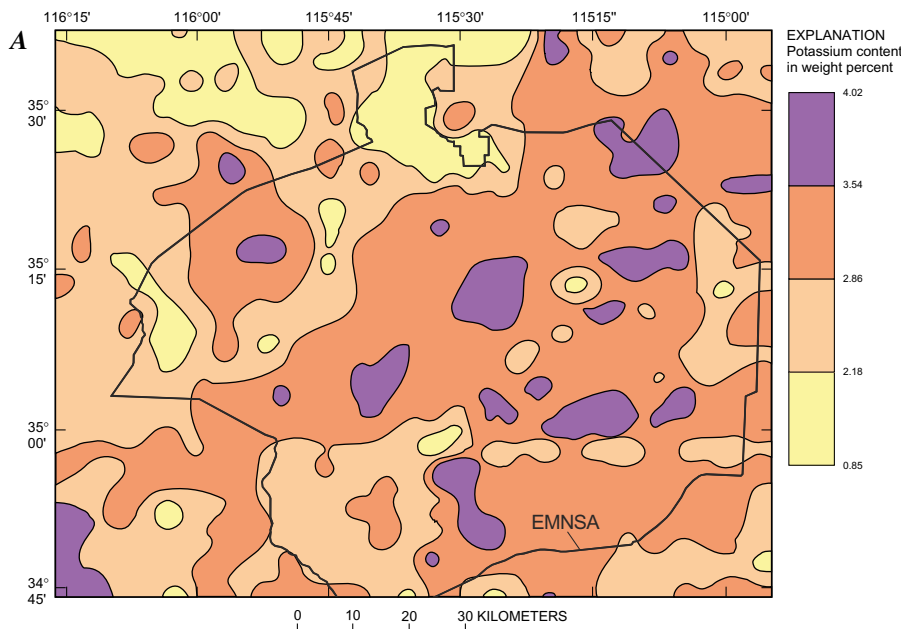


Figure 35. Contoured chemical-composition values, derived from aerial gamma-ray surveys, of rocks in area of East Mojave National Scenic Area (EMNSA, outlined); representative data given in table 8. *A*, Potassium, in weight percent. *B*, Thorium, in parts per million equivalent. *C*, Uranium, in parts per million equivalent.

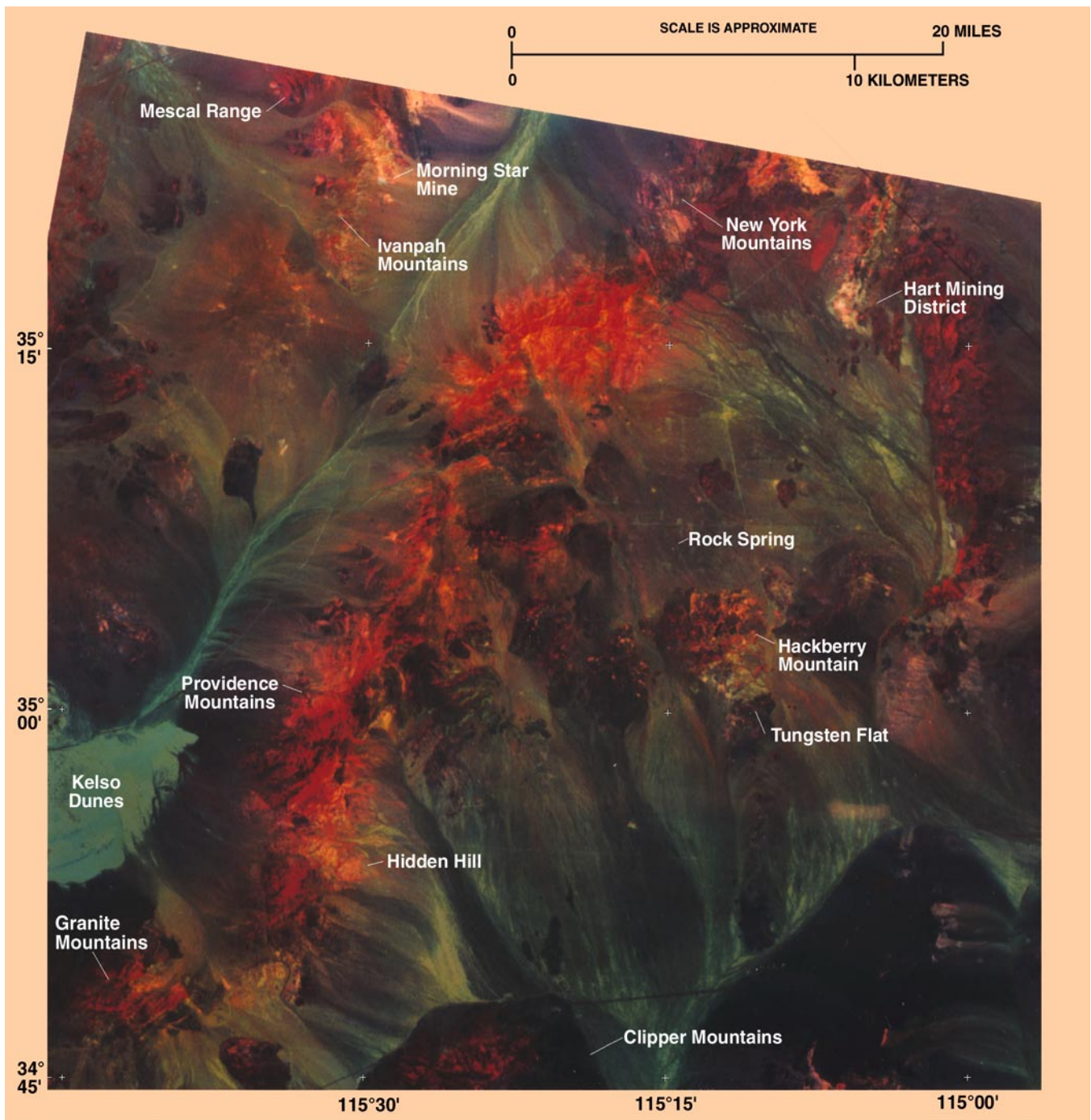


Figure 36. Color-ratio-composite (CRC) image of part of East Mojave National Scenic Area, Calif., showing significant alteration (white areas) in area of Hart Mining District (CRC image produced by digital image processing of one-quarter of Landsat Thematic Mapper scene 50 8271 73 95). Other areas of alteration appear to be located at Hidden Hill, at Hackberry Mountain, and near Morning Star Mine.

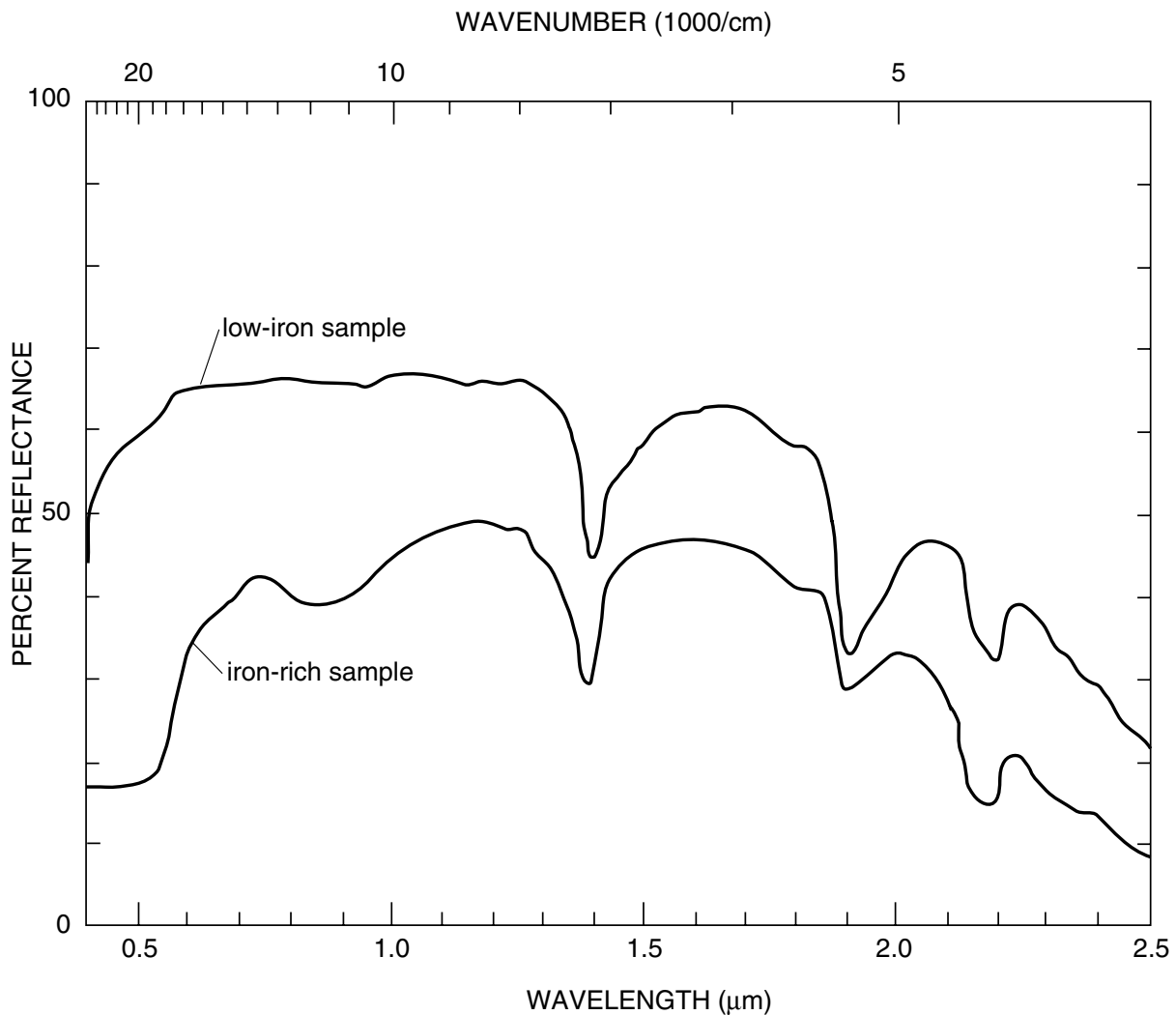


Figure 37. Spectral reflectance of two highly altered dacite-rhyolite samples collected at Castle Mountains gold deposit, Hart Mining District (fig. 2; unit Tdr, pl. 1), East Mojave National Scenic Area, Calif. For both samples, Thematic Mapper (TM) band 7 will have a low value, resulting in high TM 5:7 ratio value (red). Value of TM 3:1 ratio (green) will be high for iron-rich sample, moderate for low-iron sample; TM 3:4 ratio (blue) value will be low to moderate for the iron-rich sample, low for low-iron sample. Sum of TM ratio values will produce white-to-yellow color-ratio-composite image (fig. 36).

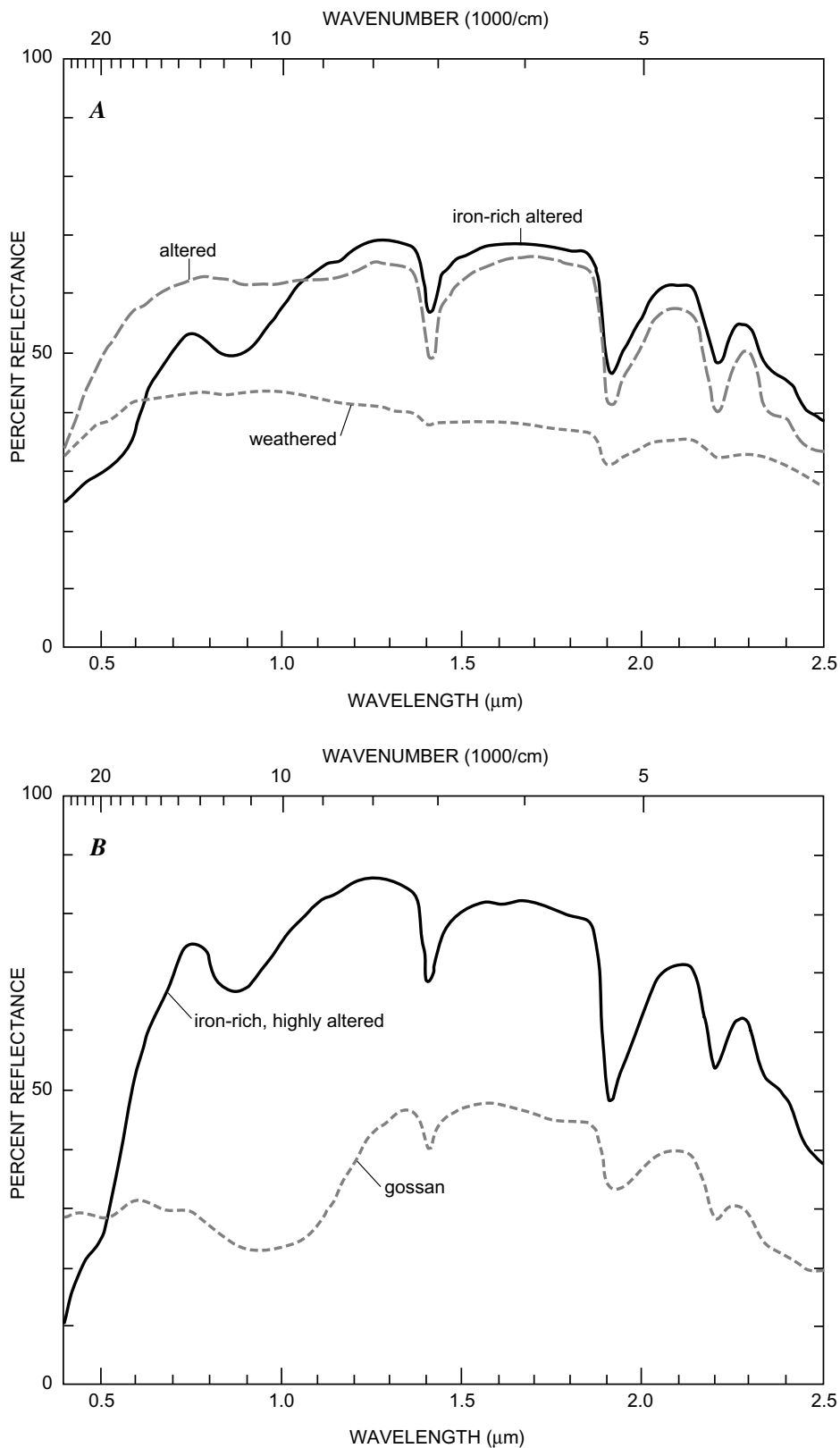


Figure 38. Spectral reflectance of samples at Hidden Hill Mine, East Mojave National Scenic Area, Calif. *A*, Spectral reflectance of weathered sample of quartz monzonite (Jgo, pl. 1), of altered sample of quartz monzonite, and of altered, iron-rich sample of quartz monzonite. Color response on color-ratio-composite (CRC) image of weathered rocks will be blue to slight magenta. *B*, Spectral reflectance of highly altered, iron-rich sample of quartz monzonite and of gossan. Altered rocks will produce yellow-to-white color on CRC image similar to white areas present at Hart Mining District (fig. 36). Value for Thematic Mapper (TM) 3:1 ratio will not be as high for gossan sample, reducing green component on CRC image.

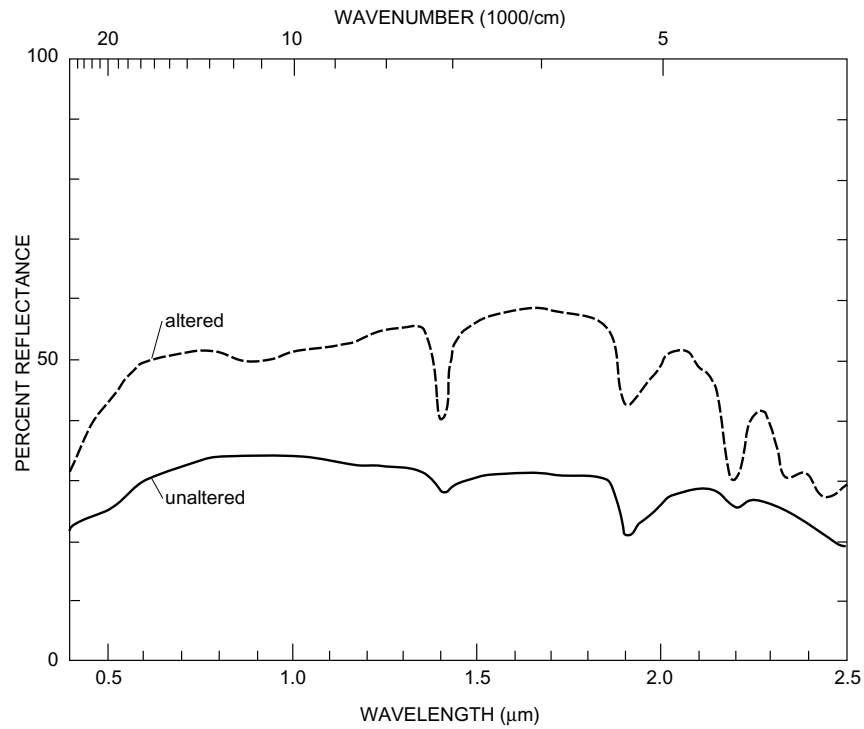


Figure 39. Spectral reflectance of altered and unaltered samples of monzogranite (unit Kg₁, pl. 1) collected at open shaft in general area of Tungsten Flat, East Mojave National Scenic Area, Calif. Color response of altered sample will be white on color-ratio-composite image (fig. 36); unaltered sample, blue to slight red.

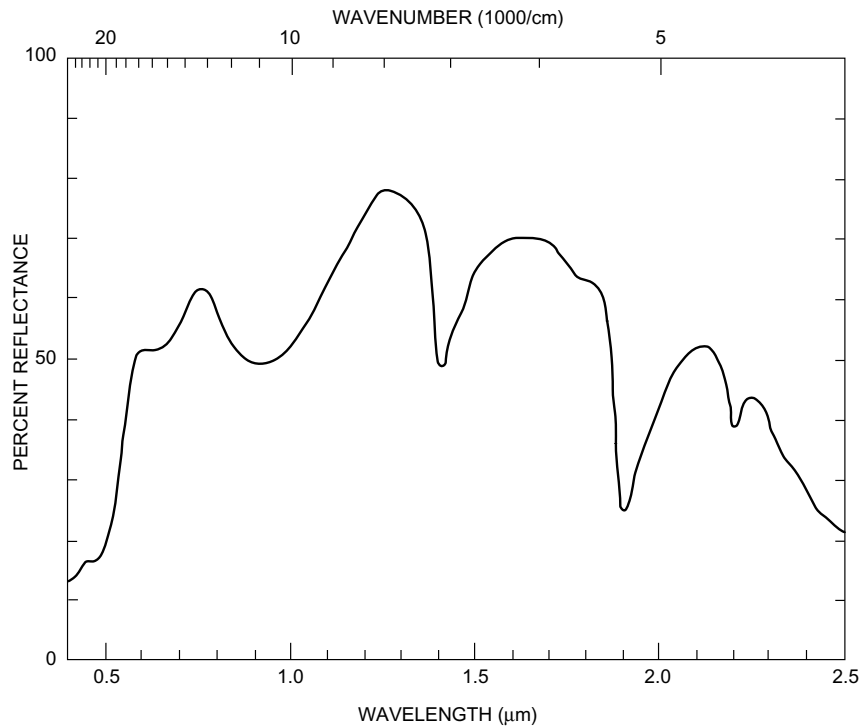


Figure 40. Spectral reflectance of sample of highly altered informally named, Rock Spring monzodiorite of Beckerman and others (1982) (unit Krs, pl. 1), East Mojave National Scenic Area, Calif. Mafic minerals have been altered to nontronite, which dominates spectrum. Color response will be white on color-ratio-composite image (fig. 36).

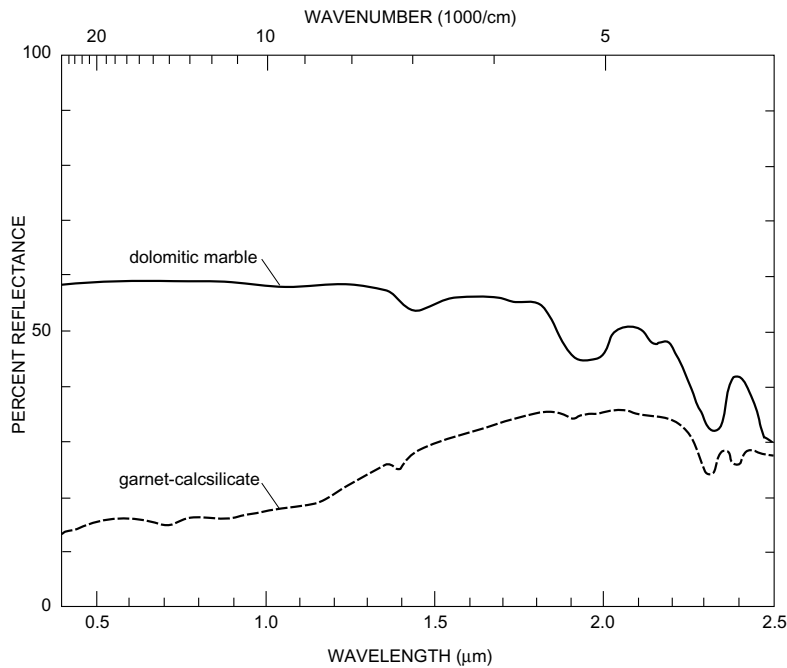


Figure 41. Spectral reflectance of samples of dolomitic marble (altered dolomite?) of Bird Spring Formation; part of unit PDI, pl. 1) and of garnet-calc-silicate rocks derived from Moenkopi Formation (unit Tm, pl. 1), both collected near skarn deposit in East Mojave National Scenic Area, Calif. Value for Thematic Mapper (TM) 5/7 ratio (red) for marble will be high, less so for calc-silicate rocks. Color response of TM 3:1 (green) and 3:4 (blue) ratio values will be low for both samples. Resultant colors on color-ratio-composite image (fig. 36) are similar but show deeper red response for carbonate-bearing rocks.

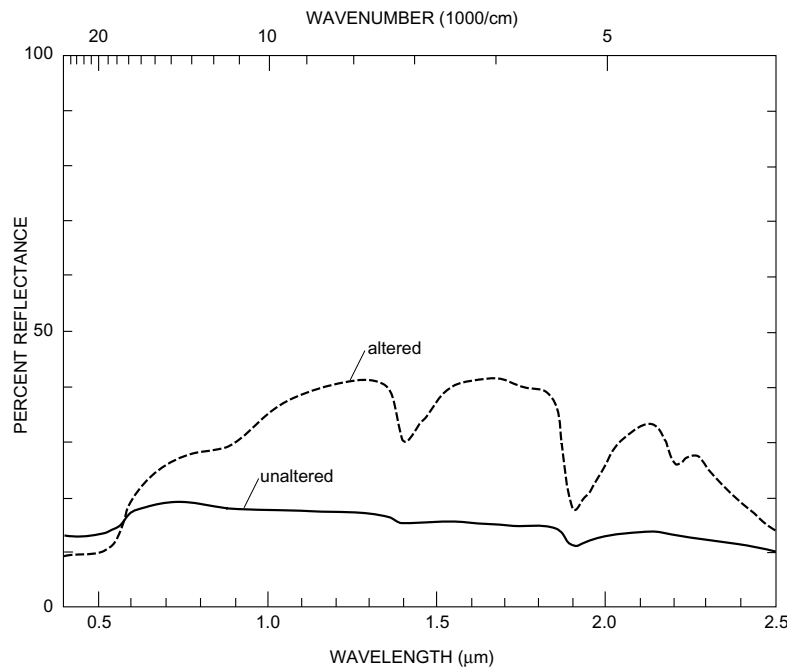


Figure 42. Spectral reflectance of altered and unaltered samples of monzogranite (unit Kg₁, pl. 1) (adamellite?), collected from road cut (old railroad grade) in New York Mountains, East Mojave National Scenic Area, Calif (fig. 36). Color response for altered rocks will be white on color-ratio-composite (CRC) image. Value for Thematic Mapper (TM) 3:1 ratio will be high owing to ferric-iron absorption of monzogranite, so otherwise-flat spectrum will result in slight cyan color on CRC image.

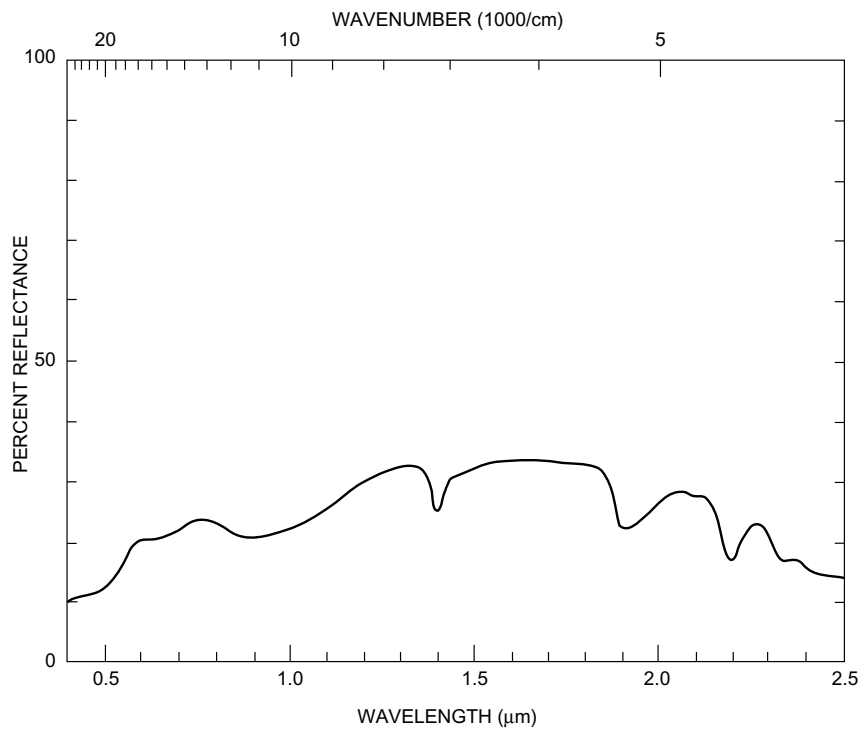


Figure 43. Spectral reflectance of sample of altered quartz monzonite (unit Jgo, pl. 1), collected at Bighorn Mine, East Mojave National Scenic Area, Calif. Resultant color on the color-ratio-composite image will be white to yellow but, as spectral reflectance is low relative to spectra exhibited on figure 36, these rocks would not be as bright on image.

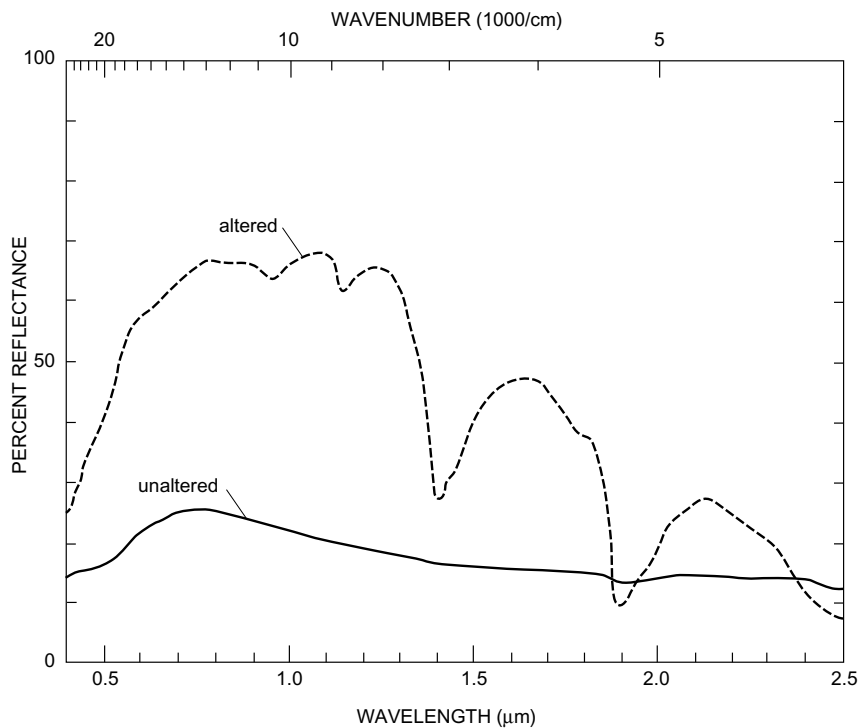


Figure 44. Spectral reflectance of altered and unaltered samples of Tertiary volcanic rocks (Peach Springs(?) Tuff of Young and Brennan (1974); unit Tps, pl. 1), East Mojave National Scenic Area, Calif. Altered sample collected north of Hackberry Mountain. Altered volcanic rocks should be very bright white but actually appear yellow on color-ratio-composite (CRC) image, possibly because of thin cover of vegetation. Unaltered volcanic rocks are blue to slight magenta on CRC image.

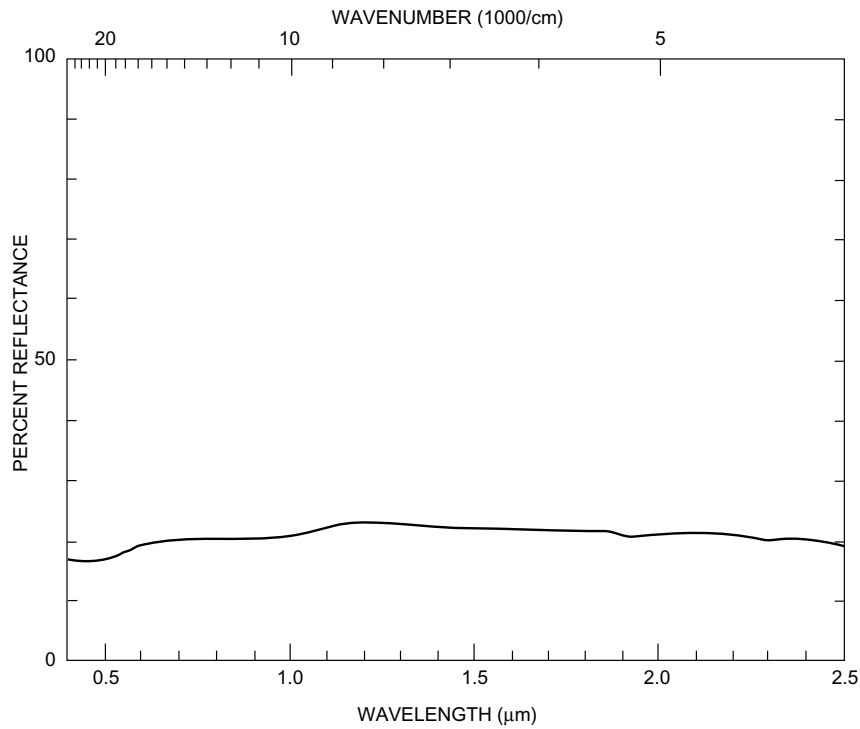


Figure 45. Spectral reflectance of altered and unaltered dacite flow-rock (unit Td, pl. 1), collected in Piute Hills, near old Mohave road, East Mojave National Scenic Area, Calif. Flat spectrum produces blue color in color-ratio-composite image.

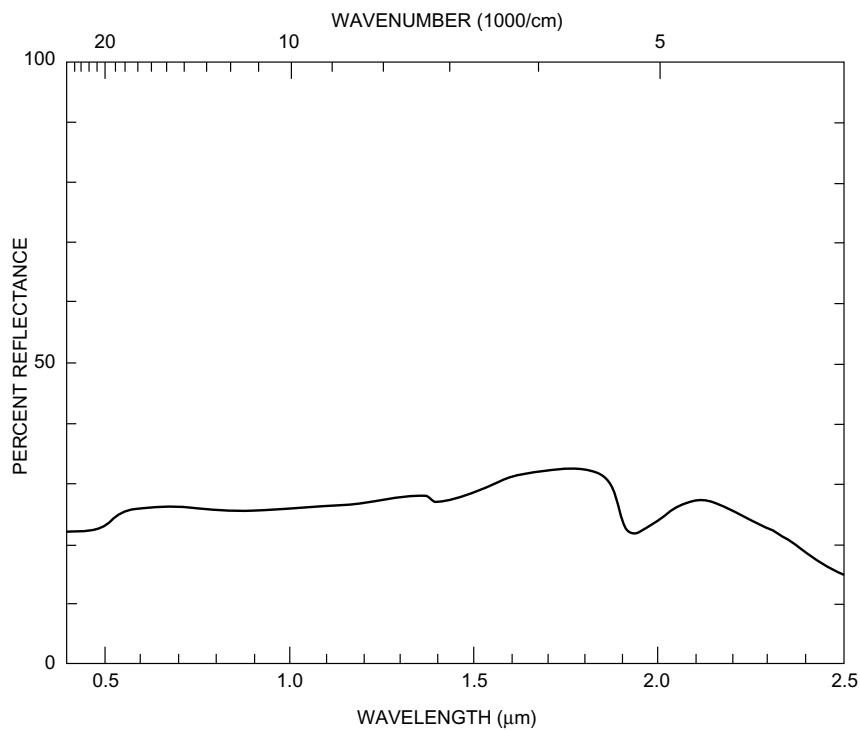


Figure 46. Spectral reflectance of sample of weathered surface of Early Proterozoic quartz diorite (unit Xg₁, pl. 1), collected near True Blue Mine. Sample does not appear to be altered. Spectrum is flat except for slight absorption in short wavelengths (Thematic Mapper (TM) band 1) owing to ferric iron on weathered surface. Color response will be blue with very slight green component on color-ratio-composite image.

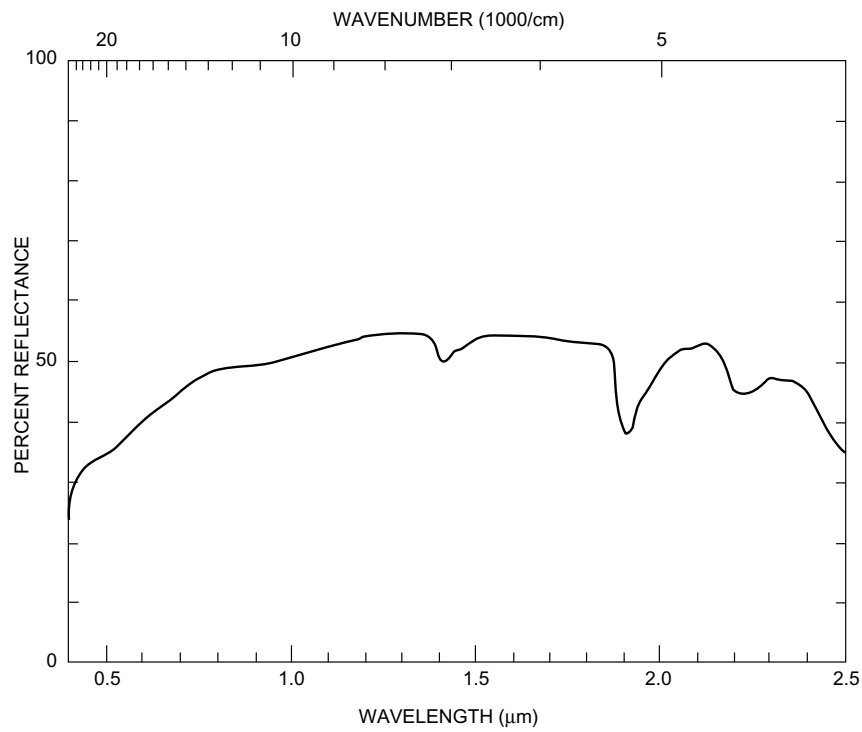


Figure 47. Spectral reflectance of sample of light-colored rhyolite ash-flow tuff (White Horse Mesa Tuff of McCurry (1988); unit Tw, pl. 1), which appears to be slightly altered; collected near Hole-in-the-Wall campground, East Mojave National Scenic Area, Calif. Spectrum of this very bright tuff displays an absorption band near 2.2 μm , resulting in high Thematic Mapper (TM) 5:7 ratio value (red), as well as moderately high TM 3:1 and 3:4 ratio values (green and blue, respectively). Unaltered rocks can be confused with altered rocks because of resulting white-to-yellow color response on color-ratio-composite image.

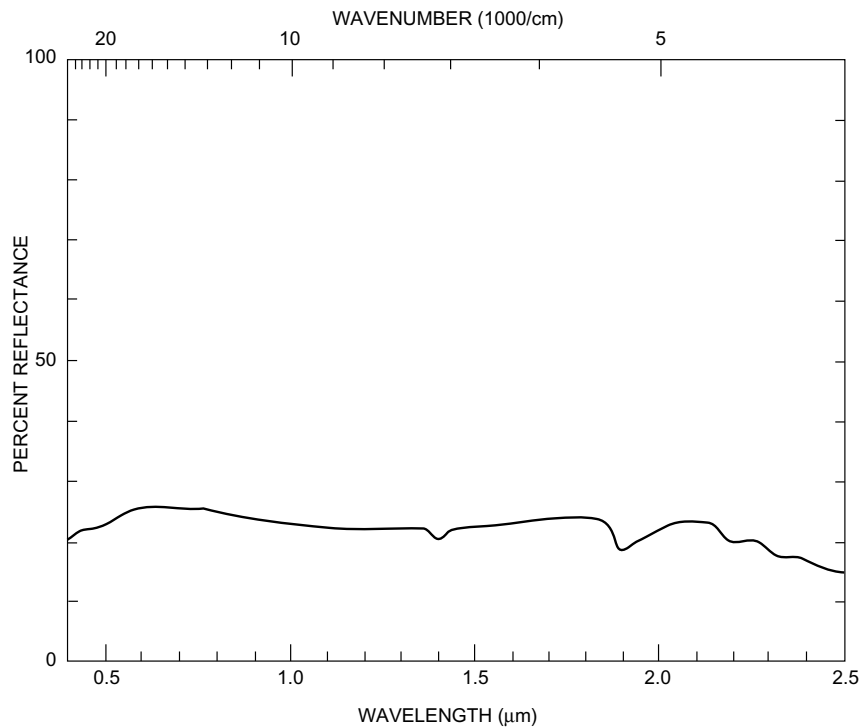


Figure 48. Spectral reflectance of sample of syenogranite (unit Jqs, pl. 1), collected at Granite Pass, East Mojave National Scenic Area, Calif. Because of 2.2-mm and 2.34-mm absorption, which is due to micaceous minerals, Thematic Mapper (TM) 5:7 ratio value (red) will be high. Weathering of biotite results in ferric-iron absorption (high TM 3:1 ratio value) and should produce green component in color-ratio-composite image. Ferric-iron band is relatively weak for most of exposed syenogranite in CRC image, resulting in blue color.

Table 8. Estimated average concentrations of potassium, uranium, and thorium, derived from aerial gamma-ray surveys, for various geologic units in the East Mojave National Scenic Area, Calif.

[Contoured data shown on fig. 35; see plate 1 for description of map units]

Map unit	Estimated Concentration values		
	Potassium (percent K)	Uranium (ppm eU)	Thorium (ppm eTh)
Qaf	2.9	3.2	13.0
Qes	2.2	2.4	.4
Qes	2.9	3.9	18.5
Qp	2.4	4.2	18.5
QTbl	1.6	2.5	8.
QTg	2.6	2.7	8.3
Td	2.2	3.	10.9
Tdr	2.1	3.9	19.5
Tg	2.7	2.4	13.
Tts	3.5	4.4	15.4
Tv ₁	3.	3.9	14.3
Tw	3.	3.5	15.
Kg ₁	2.4	2.4	10.1
Klo	2.7	2.9	7.3
Kmh	3.	2.4	13.3
Kpm	2.	3.4	12.
Krs	2.3	2.6	12.
Kt	2.8	3.4	18.9
KJg	2.4	3.4	14.5
Jd	2.3	2.5	9.5
Jcf	2.6	1.9	12.
Jg	2.1	3.1	11.5
Jgo	3.	2.9	11.5
Ji	3.2	3.4	31.
Jcm	1.9	2.8	9.
Js	2.8	2.1	6.5
Mzv	2.3	4.	11.3
€Zs	1.9	1.6	6.5
€d	.5	1.5	3.
Xg	2.5	2.8	15.2
Xg ₁	2.4	2.5	12.4
Xg ₂	3.2	3.4	14.
Xm	2.	2.1	17.5

Table 9. Summary of resultant colors of alteration minerals and vegetation on a color-ratio-composite image prepared from Landsat Thematic Mapper satellite image.

[Primary colors calculated using the following ratios: red, band 5:7; green, 3:1; blue, 3:4. Resultant color is sum of primary colors. From Knepper and Simpson, unpub. data, 1991]

Material	Primary color			Resultant color
	Red	Green	Blue	
Carbonate and hydroxyl-bearing minerals	High	Low	Moderate to low	Magenta
Limonite (hematite, goethite)	Low	High	Moderate to high	Green to cyan
Limonite (jarosite)	High	High	Moderate to high	Yellow to white
Carbonate minerals, hydroxyl-bearing minerals, and limonite	High	High	Moderate to high	Yellow to white
Vegetation	High	Low	Very low	Red